

# RELATIONSHIP OF POLYMERIC FRAGMENTS IN "BROKEN" GEL TO FORMATION PERMEABILITY REDUCTION

C. S. DeVine and R. M. Tjon-Joe-Pin  
BJ Services Company

## ABSTRACT

Although fluid viscosity reduction is commonly used to gauge polymer degradation and viscosity reduction does indicate that polymer degradation has occurred, it is misleading to conclude that reduced viscosity equates to improved fracture conductivity or retained formation permeability. Polymer fragments which result from the normal breaking of gelled, cross-linked fracturing fluids no longer contribute significantly to fluid viscosity but do contribute to proppant pack and/or formation permeability damage.

Laboratory evaluations and procedures to characterize the efficiency of gel breakers, based upon the size distribution of the generated polymeric fragments, have been presented in previous studies. Results of core flow evaluations are presented in this study, and demonstrate the relationship of typical molecular weight distributions produced by degraded typical cross-linked fracturing fluids to permeability and production reduction within the rock matrix. Several ranges of core permeability were evaluated.

Data yield a quantitative profile of the extent of formation permeability damage that can be expected based upon polymer fragment distributions and the original rock permeability. Detailed analysis of the data are provided.

## Background

The inadequate degradation of the polymers used in hydraulic fracturing fluids is known to negatively impact well productivity.<sup>1,2</sup> The addition of gel breakers to fracturing fluids is recommended to promote degradation of the polymeric filtercake and improve fracture conductivity. The breakers ideally degrade the polymer by cleaving the polymeric macromolecule into small fragments which can be produced from the fracture during load recovery. Viscosity reduction of the gelled fluid is the commonly used gauge of polymer degradation, with the assumption that the observance of a "broken gel" viscosity at the surface upon return flow is proof positive optimum gel degradation. The definition of a "broken gel" in terms of viscosity has been a moving target for several years. As recently as 15 years ago, a broken gel was defined as one having the viscosity reduced to a value of less than 15 cps as measured at  $511 \text{ sec}^{-1}$  on a Fann 35 viscometer. Subsequent to the reports of several researchers on the high degree of fracture conductivity damage caused by fracturing fluid residues, the broken gel criteria was reduced to less than 10 cps. Some stimulation engineers are today specifying that returned gels be broken to less than 5 cps.

Although viscosity reduction indicates polymer degradation, it is misleading to conclude that this reduced viscosity will equate to fracture cleanup and improved conductivity. Solution viscosity is a function of both the polymer concentration in solution and the molecular weight of the polymer. At a given constant concentration, solution viscosity exhibits an exponential relationship with the molecular weight of the polymer used to viscosify the fluid.<sup>3</sup> Cleavage to reduce the polymeric molecular weight results in an exponential reduction in the solution viscosity. Guar solutions broken at 160°F with an oxidative breaker to a viscosity of 3 cps have been reported to have average polymer molecular weights in the range of 250,000 to 500,000, with about 20% of the polymer remaining essentially unbroken at a molecular weight of greater than 2 million.<sup>4</sup> Viscosity reduction may also occur due to the creation of insoluble polymeric fragments by undesirable reactions. The polymer fragments which are desolubilized from the gelled fluid no longer contribute to fluid viscosity but do, unfortunately, contribute significantly to proppant pack damage.

Several authors have previously discussed the results of various laboratory studies to evaluate the molecular weight reduction of fracturing fluid polymers and breaker performance.<sup>4-7</sup> Almond investigated the factors effecting gelling agent residue and the relative effects of break mechanisms on flow impairment at low temperatures.<sup>5,6</sup> Almond observed that broken fracturing gels can cause significant flow reduction in porous media and that the break temperature or break mechanism plays an important role in determining the amount of flow impairment obtained with guar polymers. Volk and Gall et.al. reported on molecular size studies of degraded fracturing fluids in conjunction with the DOE Multi-Well Experiments in the mid-80's.<sup>3,4</sup> The work was very insightful, utilizing Size Exclusion Chromatography to relate the relative average molecular weight reduction with the effects on fluid viscosity. They observed that degradation of the fluid viscosity did not ensure fluid return because the broken fluids contained sufficient partially degraded residues to damage and restrict the fracture permeability. They also confirmed that the viscosities of the degraded solutions were functions of polymer concentration and molecular weight and derived a correlation between the log of the polymer average molecular weight and the inverse of the solution viscosity.

Previous studies in this laboratory have concentrated on the efficiency of various breakers in the molecular weight reduction of crosslinked and uncrosslinked guar-based fluids. Extensive testing demonstrated that conventional enzyme breakers provided more efficient molecular weight reduction than did oxidizers and activated oxidizers, but Guar-Linkage-Specific Enzyme breakers outperformed conventional enzyme and oxidative breakers.<sup>8,9</sup>

The current study was initiated to determine the effect of broken fluids with varying molecular weight distributions on formation permeability and to determine if damage to the rock matrix permeability is the same for rocks of various permeabilities. In the first series of experiments, different breakers were compared to determine the appropriate breaker for use in additional, more extensive, studies.

## Test Rock Characterization

Three sets of samples, representing three permeabilities {"permeable", "intermediate", and "tight"}, were selected for analysis. Features of selected samples are illustrated in Figures 1 through 4, and the mineralogic analysis is given in Table 1.

**Rock Properties - Mineralogy.** Samples are very fine to upper fine grained poorly to moderately well sorted sandstones. Quartz is the principal mineral phase in all samples. Plagioclase feldspar is moderately abundant in the "tight", very fine grained sample. Potassium feldspar is present in the "intermediate" permeability sample and in the "tight" sample. Calcite and dolomite were detected in minor quantities in most samples. Pyrite is present in "intermediate" and "tight" samples. Illite (mica) is abundant in the "tight" sample and was the only clay mineral detected in the sample. Illite-smectite (20% expandable smectite layers) and kaolinite are clay minerals present in greater than a trace amount in the "intermediate" permeability sample. Kaolinite and chlorite are present in greater than a trace quantity in the "permeable" sample. Thin section examination (Figures 1 through 4) reveals that patchy dolomite cement occurs in the "permeable" sample (Figure 1). Kaolinite locally fills large areas of the pore system, and may have partially replaced feldspar grains (Figure 2). Some grains have been replaced by chlorite clay. Silica (quartz) overgrowths tightly cement some portions of the "permeable" sample. The "intermediate" permeability sample is laminated (Figure 3). Calcareous skeletal fragments are present. The sample is poorly sorted. Kaolinite locally fills pores and has precipitated in interiors of skeletal tests. The "tight" sample is a lower very fine grained sandstone. Authigenic and depositional illite is present. The "tight" sample is micaceous. Carbonate cement is locally present (Figure 4).

**Rock Properties - Reservoir Quality.** Porosities were measured using a standard Boyle's Law dual cell porosimeter. Dry nitrogen permeabilities were measured by flowing dry nitrogen gas through core plugs at 400 psi overburden pressure. Average porosities ranged from 14.9% to 17.4%. Average dry nitrogen permeabilities of test rocks used in this study ranged from 0.09 md to 220 md (Table 2).

## Test Procedures

**Fluid Description.** Guar systems were used in this study. Polymer at a loading of 40 lb/1000 gallons was hydrated in deionized water. The pH of fluids used in this study was 7.8. A zirconium cross-linker was used.

Two enzyme breakers were used. A loading of 1 gal/1000 gal of Guar-Linkage-Specific Enzyme (Enzyme A) was used in all systems tested. Enzyme B is a conventional enzyme breaker and was used at a loading of 0.15 lb/1000 gal in all systems tested. Ammonium persulfate oxidative breaker was used at a loading of 0.25 lb/1000 gallons.

Breaker loadings were held constant to ensure that a fairly constant molecular weight distribution would be generated for preliminary testing.

**Fluid Preparation.** Polymer was hydrated in deionized water in 1 liter batches. Each batch was split into 4-250 mL aliquots. The prescribed quantity of breaker was added to three splits. The fourth split was retained as a control. Fluids were cross-linked and appropriate chemicals were added. The quantity of breaker added dictated the final molecular weight distribution (within statistical limits) of the fluid to be injected into the core. Fluids were used within 72 hours of preparation.

**Viscosity Measurement.** The pretest viscosity was measured with a Fann 35 with a R1:B1 rotor:bob configuration at 300 rpm which yields a fluid viscosity at  $511 \text{ sec}^{-1}$ . This measurement is standard for the evaluation of broken gel viscosity. The initial viscosity of the unbroken gel was 100 cp. Viscosities were measured after fluid breaking but before core injection. The viscosity of effluent liquid from each core flow was tested.

**Molecular Weight Distribution.** Molecular weight distributions were determined both before and after fluid flow through core plugs, using an Ultra-Filtration Molecular Weight cut-off technique. Separation of the variously sized polymer fragments in broken gel solutions is achieved by filtration of the bulk fluid across semi-permeable membranes using centrifugation. Fragments which are too large to pass through the membrane are trapped on the membrane surface. Calibrated Millipore Ultrafree-CL membranes were used. Cutoff membranes utilized in this study were selected to separate fragments to 1200K, 300K, 100K, 30K, 10K, and 5K molecular weights. Membranes were flushed with deionized water and centrifuged before the addition of each sample. Each membrane tube was weighed prior to sample addition and was weighed again after centrifugation to determine the weight of polymer trapped on the membrane. The total is determined and the distribution is calculated as a percentage of fragments falling between successively sized membranes.

**Flow Testing.** Four two inch in length and 1 inch in diameter plugs were drilled from each of the three selected core sections. One plug from each set of four plugs was reserved for further analysis. Plugs were cleaned using vapor extraction. Prior to oil flow, cores were saturated with potassium chloride water, containing a mutual solvent and a strongly water wetting surfactant. Plugs were mounted in rubber sleeves and sealed with a confining pressure of 2000 psi. One apparatus used in testing is illustrated in Figure 5. Synthetic oil injection was continued until steady state permeability was achieved. Broken fracturing fluid was injected into each core, and the effluent was collected until a volume adequate for post-flow molecular weight testing and viscosity testing was obtained. The post-flow viscosity and post-flow molecular weight distribution was determined for each test. Flow was continued in the forward direction until steady state permeability was achieved.

## Results and Discussion

**Flow testing.** Results of flow tests pertinent to the current study are given in Table 3 for "permeable" rocks and in Table 4 for "tight" rocks. Features of two samples are illustrated in Figures 6 and 7, to demonstrate the pre-test and post-test appearance of these samples.

Permeability reduction is greater for "permeable" rocks than for "tight" rocks. The permeability reduction also appears to be related to the type of breaker utilized to prepare injection fluids. In the permeable rock case, fluid broken with Enzyme A provided the least damage to the permeability. Contact of cores with fluids broken with the oxidizer resulted in the greatest loss of permeability. Oxidizer damage, however, was the result of both polymer fragment trapping in the pore system and the secondary precipitation of iron oxides (hydroxides). The APS was slightly better than Enzyme A in tight rock testing. Note that penetration of fragments in tight rocks will be limited by reservoir characteristics. The plug used in the oxidizer test was about 30% less permeable than was the plug used in the Enzyme A test. Less fragment penetration would be anticipated for the tighter sample, with damage perhaps being less than for the slightly more permeable plug.

Specifically, the steady state permeability of one "permeable" core plug, flowed with fluid broken with Enzyme A, was reduced from 156 md to 68 md (44% regain); the permeability of a second "permeable" core plug, flowed with fluid broken with Enzyme B, was reduced from 127 md to 41 md (32% regain); and the permeability of the third "permeable" core plug, flowed with fluid broken with APS (oxidizer), was reduced from 109 md to 32 md (29% regain). Examination of scanning electron micrographs (Figure 6) of a permeable plug before and after contact with a fluid broken by the oxidizer reveal that polymer aggregates and sheaths have draped pores and pore walls and have adhered to grain surfaces.

The steady state permeability of one "tight" core plug, flowed with fluid broken with Enzyme A, was reduced from 0.085 md to 0.071 md (84% regain); the permeability of a second "tight" plug, flowed with fluid broken with Enzyme B, was reduced from 0.081 md to 0.053 md (65% regain); and the permeability of the third "tight" plug, flowed with fluid broken with the oxidizer, was reduced from 0.068 md to 0.060 md (88 % regain). Examination of comparative sections of pre- and post-test chips with the scanning electron micrograph (Figure 7) reveals that polymer was apparently unable to invade the rock pore system, thus accounting for the lower degree of damage to tight rocks, as compared with permeable rocks. In fact, the rock pore system appears to have been "cleaned".

**Viscosity.** Pre- and post-test fluid viscosities are compared in Tables 5 - 7 for each breaker used. As anticipated, fluid viscosities after flow through the core are less than pre-test fluid viscosities. Pre-test fluid viscosities ranged from 2.3 cp to 4.0 cp. Post-flow viscosities are generally 1.2 cp to 1.4 cp.

**Molecular weight distribution.** Results of pre-flow and post-flow molecular weight distributions are given in Table 8 and are displayed in Figures 8 - 13. Pre-flow and post-flow distributions for each test are illustrated on the same graph for ease of comparison.

Results for permeable core plug tests generally show that the >1200K fraction is reduced in post-flow samples. The reduction is slight for the oxidative breaker (Figure 10), and is nearly complete for the Enzyme A breaker test (Figure 8). Distributions were, most probably, not significantly affected since many polymer fragments are small enough to pass through the pore system. Results for tight core plug tests, however show that a significant quantity of the higher molecular weight fraction is removed. For the Enzyme A test, The dominant size fraction is >1200K before injection into the core. After injection, the 10K to 30K fraction is dominant (Figure 11). The test with the oxidative breaker (Figure 13) shows the same trend. Clearly, the noted effect is not due to the breaker system used but is due to the natural filtering action of small pores and narrow pore throats. Large polymer fragments could not penetrate the pore system.

## Conclusions

1. The rock matrix of permeable zones (100 - 200 md) is damaged by the flow of fluids containing high molecular weight polymer fragments. Viscosities of all pre-flow fluids used were less than 5 cp.
2. Permeability damage to "permeable" rocks occurred as a result of large fragments bridging pore throats and pores and providing sites for further fragment accumulation.
3. "Permeable" plugs were more damaged than were "tight" plugs.
4. Permeability damage to "tight" rocks occurred as a result of pore and pore throat plugging on the injection face of the plug. Much of the damage was removed during flowback. Solids were observed during flowback.
5. Additional damage resulted from the contact of fluids containing oxidative breakers with iron bearing mineral phases (chlorite, illite, possibly pyrite) in cores. Oxidation of iron was observed only in those tests involving the oxidative breaker.

## References

1. van Poolen, H.K., Tinsley, J.M., and Saunders, C.D.: "Hydraulic Fracturing - Fracture Flow Capacity vs. Well Productivity," JPT (May 1958) 91-95; Trans, AIME, 213.
2. Tannich, J.D.: "Liquid Removal From Hydraulically Fractured Gas Wells," JPT (November 1975) 1309-1317.

3. Volk, L.J., Gall, B.L., Raible, C.J., and Carroll, H.B.: "A Method for Evaluation of Formation Damage Due to Fracturing Fluids," paper SPE/DOE 11638 presented at the 1983 SPE/DOE Symposium on Low Permeability, Denver, CO, March 14-16.
4. Gall, B.L. and Raible, C.J.: "Molecular Size Studies of Degraded Fracturing Fluid Polymers," paper SPE 13566 presented at the International Symposium on Oilfield and Geothermal Chemistry, Phoenix, AZ, April 9-11, 1985.
5. Almond, S.W.: "Factors Affecting Gelling Agent Residue Under Low Temperature Conditions," paper 10658 presented at the SPE Formation Damage Symposium, Lafayette, LA, March 24-25, 1982.
6. Almond, S.W. and Bland, W.E.: "The Effect of Break Mechanisms on Gelling Agent Residue and Flow Impairment in 20/40 Mesh Sand," paper SPE 12485 presented at the SPE Formation Damage Control Symposium, Bakersfield, CA, February 13-14, 1984.
7. Hawkins, G.W.: "Molecular Weight Reduction and Physical Consequences of Chemical Degradation of Hydroxypropyl Guar in Aqueous Brine Solutions," Proc. ACS Division of Polymer Materials: Science and Engineering (1986) 55.
8. Brannon, H.D. and Tjon Joe Pin, R.M. : "Characterization of Breaker Efficiency Based upon Size Distribution of Polymeric Fragments," paper SPE 30492 presented at the 70th SPE Annual Technical Conference and Exhibition, Dallas, TX, October 22-25, 1995.
9. Brannon, H.D. and Tjon Joe Pin, R.M. : "Characterization of Breaker Efficiency Based Upon Size Distribution of Polymeric Fragments Resulting from Degradation of Crosslinked Fracturing Fluids," paper SPE 36496 presented at the SPE 71st Annual Technical Conference and Exhibition, Denver, CO, October 6-9, 1996.

### **Acknowledgments**

The authors wish to express our appreciation to the management of BJ Services Company for permission to pursue and publish this research and to Helena Yang and Kim Nessler for their contributions toward gathering the data necessary for this study.

Table 1  
Mineralogic Composition of Test Samples

MINERAL PHASE	APPROXIMATE WEIGHT %		
	Permeable	Intermediate	Tight
ILLITE-SMECTITE *	Tr	5	ND
ILLITE (AND/OR MICA)	Tr	Tr	12
KAOLINITE	1	4	ND
CHLORITE	1	ND	ND
CALCITE	ND	2	1
DOLOMITE	Tr	Tr	2
QUARTZ	97	84	65
PLAGIOCLASE FELDSPAR	ND	ND	14
POTASSIUM FELDSPAR	ND	2	4
PYRITE	ND	2	1
GYPNUM	ND	Tr	ND
* THE ILLITE-SMECTITE CONSISTS OF 80% ILLITE LAYERS AND 20% SMECTITE LAYERS. Tr = <1% ND = NOT DETECTED			

Table 2  
Average Porosity/Permeability Characteristics

SAMPLE	Porosity, %	Dry N <sub>2</sub> Permeability, md
"Permeable"	17.4	220
"Intermediate"	17.2	10
"Tight"	14.9	0.09

Table 3  
Steady State Permeability Before and After Treatment  
"Permeable" Samples

BREAKER	Initial Permeability, md	Final Permeability, md	% Regain
Enzyme A	156	68	44
Enzyme B	127	41	32
Oxidizer	109	32	29

Table 4  
Steady State Permeability Before and After Treatment  
"Tight" Samples

BREAKER	Initial Permeability, md	Final Permeability, md	% Regain
Enzyme A	0.085	0.071	84
Enzyme B	0.081	0.053	65
Oxidizer	0.068	0.060	88



Table 5  
Viscosity Before and  
After Treatment - Enzyme A

SAMPLE	Viscosity, cp (Before)	Viscosity, cp (After)
"Permeable"	3.0	1.2
"Tight"	2.3	1.2

Table 6  
Viscosity Before and  
After Treatment - Enzyme B

SAMPLE	Viscosity, cp (Before)	Viscosity, cp (After)
"Permeable"	2.5	1.4
"Tight"	2.5	1.4

Table 7  
Viscosity Before and After Treatment - Oxidizer

SAMPLE	Viscosity, cp (Before)	Viscosity, cp (After)
"Permeable"	4.0	1.8
"Tight"	3.0	1.4

Table 8  
Molecular Weight Distributors

Test	Breaker	>1200K	300K- 1200K	100K- 300K	30K- 100K	10K- 30K	5K- 10K	<5K
1 (Before)	Enzyme A	58.4	9.1	0.8	2.0	12.4	10.8	6.5
1 (After)	Enzyme A	3.4	58.9	1.0	0.5	14.6	14.4	7.2
2 (Before)	Enzyme B	66.5	5.6	0.7	1.8	19.2	5.4	0.8
2 (After)	Enzyme B	44.8	20.0	3.2	0.1	24.3	4.0	3.6
3 (Before)	Oxidizer	82.0	0.0	0.4	0.4	12.5	1.7	3.0
3 (After)	Oxidizer	77.0	0.6	0.1	0.4	16.5	5.4	0
4 (Before)	Enzyme A	62.0	6.8	0.9	2.2	6.3	15.8	6.0
4 (After)	Enzyme A	1.1	0.3	0.0	0.8	77.6	7.7	12.5
5 (Before)	Enzyme B	69.2	3.6	1.9	1.4	4.4	13.7	5.8
5 (After)	Enzyme B	19.5	41.6	0.7	0.3	30.1	7.6	0.2
6 (Before)	Oxidizer	79.6	0.9	0.0	1.2	0.6	13.1	4.6
6 (After)	Oxidizer	0.0	0.4	0.0	6.2	55.3	24.9	13.2
Tests 1, 2, and 3 involved permeable rock. Tests 4, 5, and 6 involved tight rock Distributions are expressed as percentages by weight.								

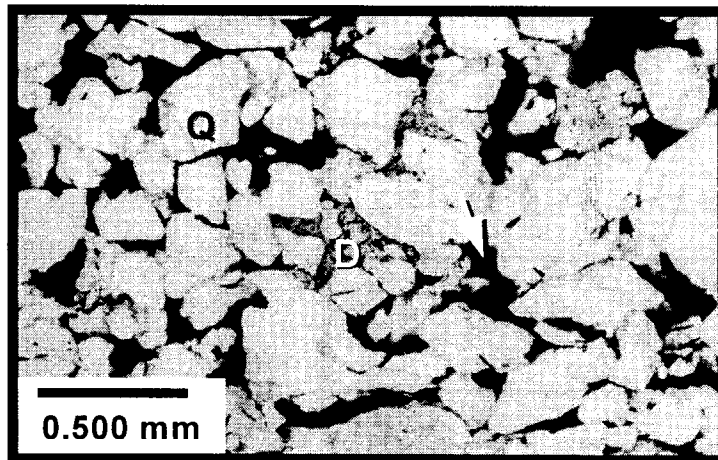


Figure 1 - Compositional and textural features of the permeable sample are illustrated. Quartz (Q) is the principal framework grain. Dolomite (D) cement is sparsely distributed in the pore system. Pores (arrow) are locally 250 microns in long dimension. 40x.

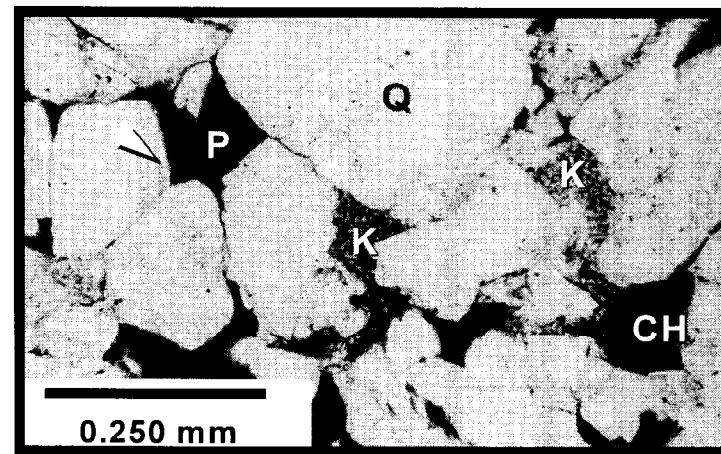


Figure 2 - The distribution of clay minerals kaolinite (K) and Chlorite (CH) are illustrated in this view of the permeable sample. Open Pores (P) are 125 microns in maximum long dimension. Silica overgrowth (arrow) have formed on quartz (Q) grains. 90x.

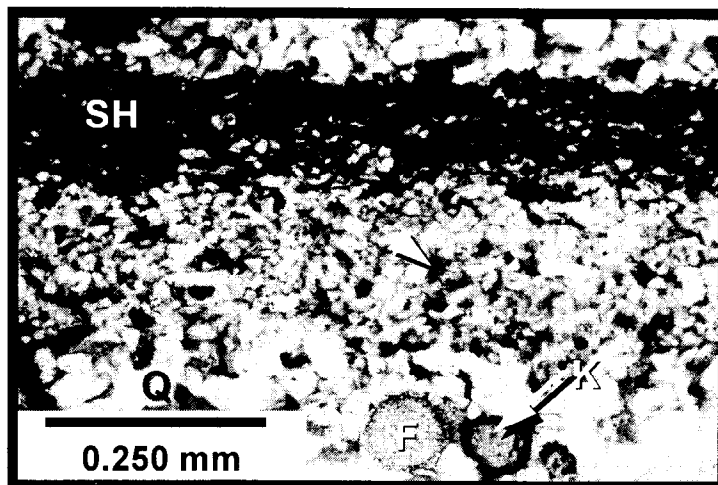


Figure 3 - Depositional shale (SH) occurs in laminations in the intermediate perm sample. Fossil fragments (F) are present, and kaolinite (K) locally fills skeletal tests. Quartz (Q) grains are fine sand to silt sized. Pores (arrow) are about 20 microns in diameter in fine grained portions of the sample. 40x.

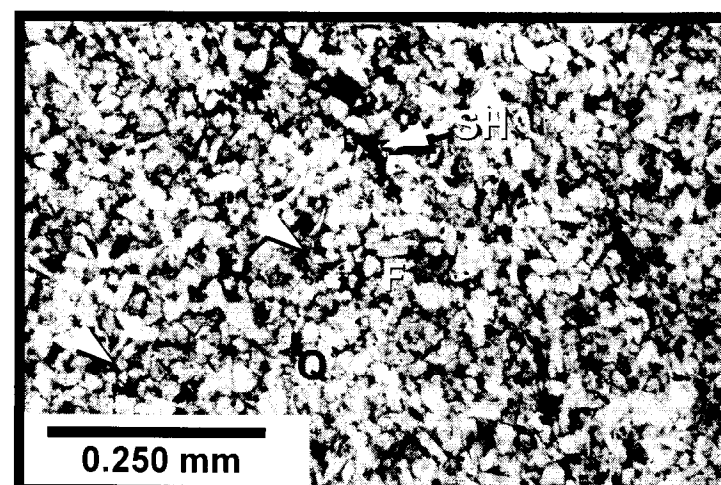


Figure 4 - The tight sample in a shaly sandstone or siltstone. Shale (SH) is dispersed in the pore system. Quartz grains (Q) are locally cemented by silica overgrowths. Feldspars (F) are moderately abundant in this sample. Open pores (arrows) are <10 microns in diameter. Carbonate fragments are present. 40x.

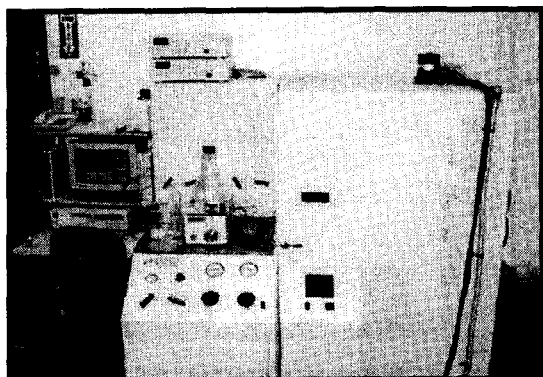


Figure 5 - An automated data collection permeameter was utilized in several tests.

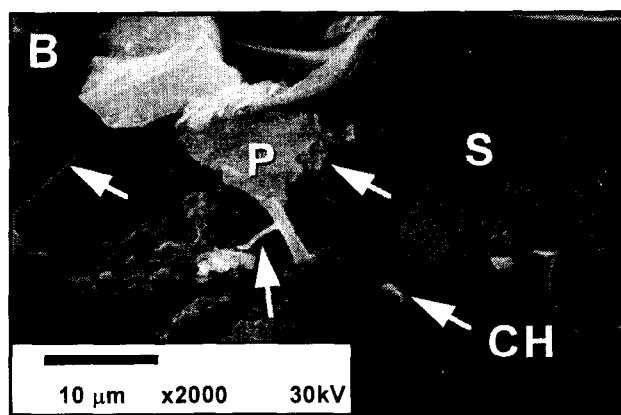
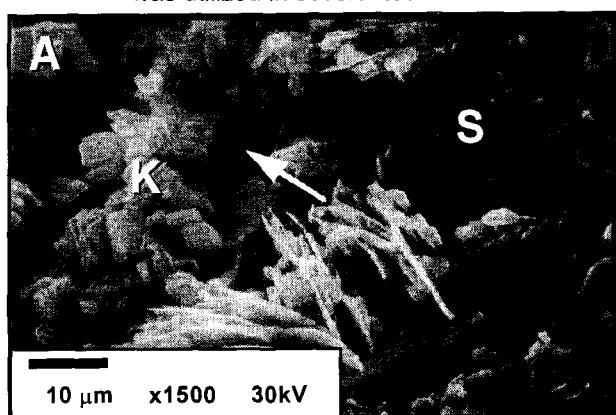


Figure 6 - Before (A) and after (B) scanning electron micrographs of the "permeable" core illustrate the accumulation of polymer (P and unlabeled arrows on photo B) in the rock. Silica (S) is the dominant cement. Chlorite (CH) and kaolinite (K) clay are well illustrated. Micropores (arrows, photo A) are present and will be readily clogged by polymer.

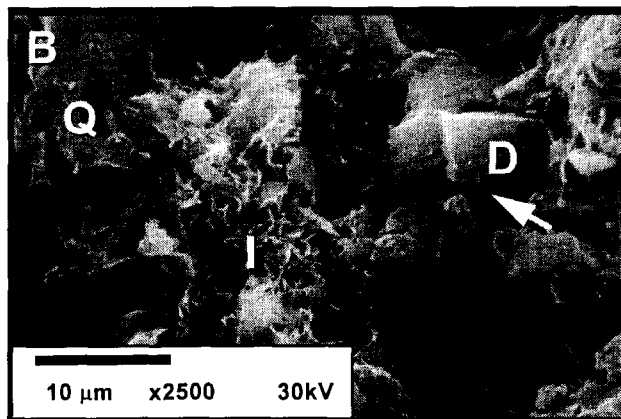
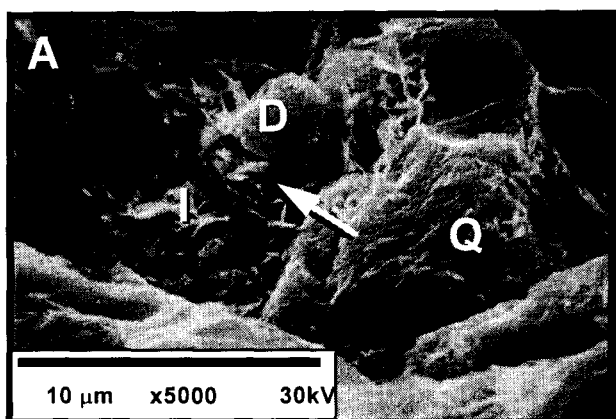


Figure 7 - Before (A) and after (B) scanning electron micrographs of a "tight" plug show that polymer accumulation is not evident. Micropores (arrows) are about 1 micron in diameter and are clear. Quartz (Q) is the principal grain, illite (I) is the principal clay, and dolomite (D) is the principal carbonate.

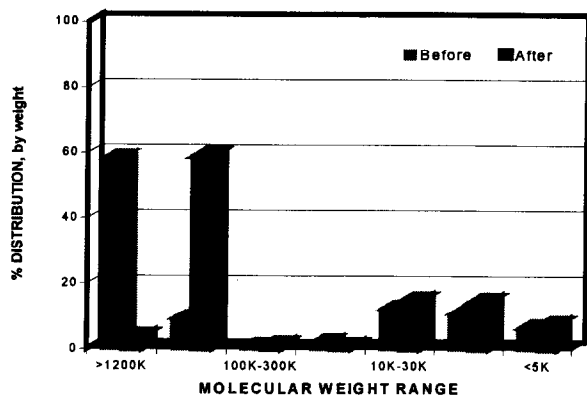


Figure 8 - Before and after molecular weight distributions of the fluid with Enzyme A tested with the "permeable" core. Note that after flow, the principal size was 300 - 1200k.

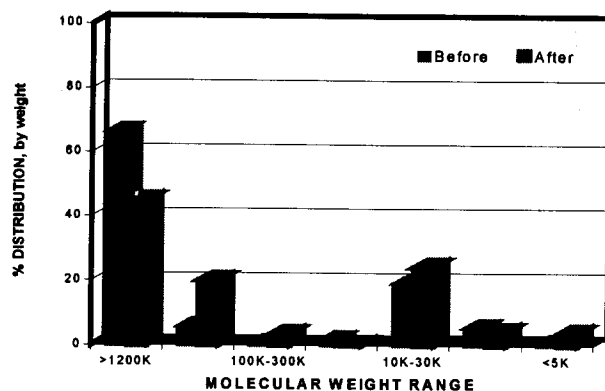


Figure 9 - Before and after molecular weight distributor of the fluid with Enzyme B tested with the "permeable" core. Distributions are similar for both fluids.

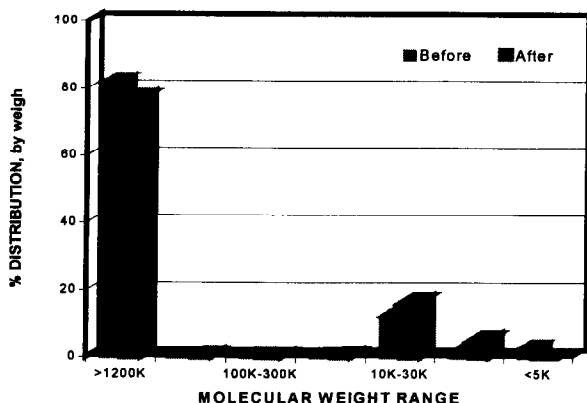


Figure 10 - Before and after molecular weight distributions of the fluid with the oxidizer tested with the "permeable" core. Distributions are very similar for both tests.

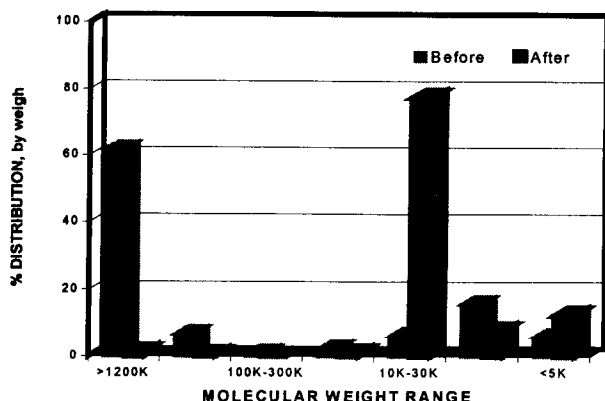


Figure 11 - Before and after molecular weight distributions on the Enzyme A test with the "tight" core. A radical shift has occurred in the distribution, indicating that the core is an effective filter.

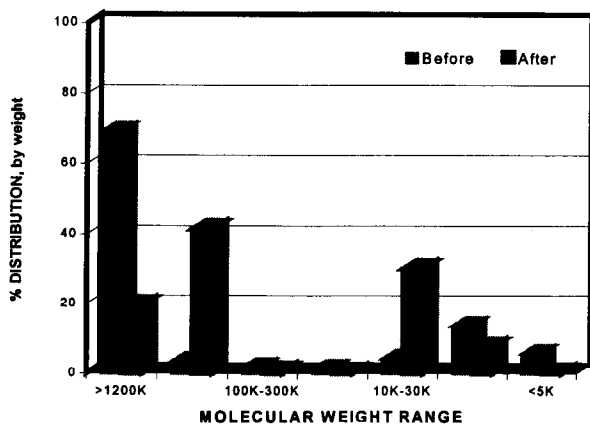


Figure 12 - Before and after molecular weight distributions of the fluid with Enzyme B tested with the "tight" core. The somewhat random nature of the distribution may indicate that the test is invalid.

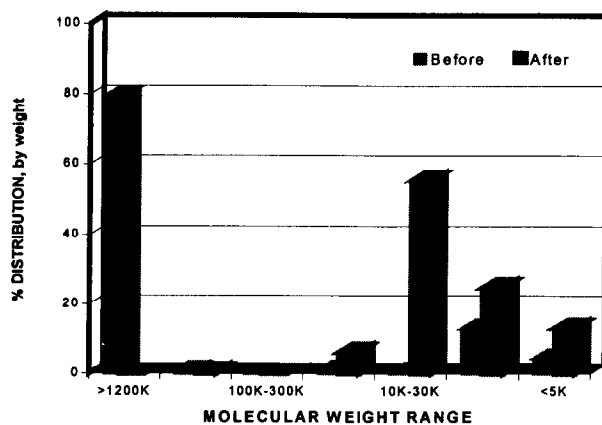


Figure 13 - Before and after molecular weight distributions of the test with the "tight" core and the oxidizer. A radical shift has occurred in the distribution, indicating that the core is an effective polymer fragment filter.